Catalysis Letters 38 (1996) 63–72

NO + H_2 reaction on Pt–Ru/SiO_2 catalysts: correlation between nanostructure and catalytic activity and selectivity

Gabriela Díaz, Antonio Gómez-Cortés and Mohamed Benaissa

Instituto de Física, Universidad Nacional Autónoma de México, PO Box 20-364, Mexico 01000, Mexico

Received 3 August 1995; accepted 8 December 1995

Nitric oxide reduction by hydrogen has been studied on Pt–Ru/SiO_2 catalysts of various Pt/Ru atomic compositions in the temperature range 298–673 K. Physical characterization showed the presence of bimetallic particles which tend to be Pt-rich. The overall activity of the bimetallic catalysts suggests a dilution of the active component (Pt) in the range 373–523 K. The addition of Ru results in a general improvement of the N_2 selectivity and significant modifications in the product distribution are observed as a function of the catalyst composition. A bimetallic particle model is proposed in which various types of surfaces are exposed including those with pure Pt atoms and/or Pt–Ru mixture. This model allows to explain the overall activity and selectivity in the whole series of catalysts.

Keywords: NOx reduction; bimetallic catalysts; HREM

1. Introduction

Reduction of nitrogen oxides by catalytic means is one of the most important reactions currently under research. Several supported metal catalysts are active for conversion of NOx to N_2 using H_2 as the reducing agent. Ru has been shown to be the most selective for reduction of NOx to N_2, while Pt is much more active but less selective [1]. In some instances, ammonia and nitrous oxide are produced as undesirable side products, but the main problem with Ru-containing catalysts for the NOx reduction under a net excess of oxygen has been associated with the volatility of ruthenium oxides [2].

The use of bimetallic catalysts for the reduction of nitric oxide has shown dual functionality and synergistic effects for several bimetallic combinations [3]. On the other hand the presence of multimetallic particles (Pt, Pd, Rh) on both fresh and aged catalysts involved in catalytic converters has been also documented [4,5]. The occurrence of multimetallic particles in a catalyst is significant because surface enrichment of one or more of the noble metals may occur, and this situation may have some influence on the catalytic performance of the sample.

It has already been shown that truly Pt–Ru bimetallic particles can be obtained when preparing supported Pt–Ru catalysts [6]. Selectivity and activity changes were observed for this system in hydrocarbon reactions, which were correlated to the presence of Pt–Ru dual sites.

The aim of this fundamental work is to investigate the influence that the addition of ruthenium has on the catalytic properties of platinum for the nitric oxide reduction by hydrogen (non-oxidizing conditions) in the range of 273–673 K. The formation, the structural and morphological features of bimetallic Pt–Ru particles were investigated by means of high-resolution transmission electron microscopy (HRTEM) and later correlated with the catalytic performance.

2. Experimental

2.1. *Catalysts preparation*

A series of bimetallic catalysts were prepared using $Pt(AcAc)_2$ and $Ru(AcAc)_3$ as precursors (Aldrich). The support was a Silica Cab-O-Sil M-5 having a BET surface area of 200 m^2/g. The samples were prepared by incipient wetness impregnation and the total metal loading was targeted at 1.5 wt%. Prior to catalytic testing, the catalysts were reduced under hydrogen at 673 K during 2 h. The present work concerns monometallic Pt and Ru catalysts, and bimetallic Pt–Ru catalysts. The latter had Pt/Ru atomic ratios of 3.0, 1.0 and 0.33, which are denoted as $Pt_{75}Ru_{25}$, $Pt_{50}Ru_{50}$ and $Pt_{25}Ru_{75}$, respectively. Another catalyst sample was prepared as a mechanical mixture of monometallic Pt and Ru catalysts which were reduced before mixing. The Pt/Ru atomic ratio was 0.33 and this sample is denoted as PtRuMX.

2.2. *Catalyst characterization*

Mean particle size and total dispersion of the metallic phase were calculated from hydrogen chemisorption measurements performed in a conventional volumetric apparatus, and then checked by means of a conventional transmission electron microscope CTEM (JEOL 100CX). For chemisorption characterization, the samples were reactivated in situ at 673 K in flowing hydrogen and then outgassed at the same temperature prior to the chemisorption measurements at 298 K. Detailed examination of the catalyst structure was performed using a high-resolution electron microscope (JEM4000EX). Samples were supported on holey carbon-coated copper grids by standard procedures. Additional EDX microanalysis studies were performed to check the chemical composition of the bimetallic particles using a JEM2010F (200 kV) electron microscope equipped with a field-emission-gun source.

2.3. NO + H_2 reaction

The reduction of nitric oxide by hydrogen was carried out in the temperature range 298–673 K. The reaction system was a down-flow fixed-bed glass reactor, and all lines and valves were stainless steel. The reactant mixture (He 97 vol%, H_2 2 vol% and NO 1 vol%) was fed through mass flow controllers (Tylan). The NO/H_2 molar ratio was 0.5 and the space velocity 30000 ℓ/h. The catalyst sample, 0.040 g, was reactivated in situ at 673 K during 1 h in a hydrogen flow of 1 ml/s and then cooled to room temperature under the same atmosphere. The catalysts were then flushed with helium prior to admission of the reactant mixture. Reaction temperature was increased progressively using a temperature controller, and catalytic measurements at each temperature were performed at steady state.

The reaction products were detected by gas chromatography (Gow Mac Series 550P, with thermal conductivity detectors, automated injection valves and a Spectra-Physics DataJet Integrator). The NO and the N_2 were separated by using a 2 m column packed with Porapak Q, while N_2O, NH_3 and H_2O were separated using a 4 m column packed with Chromosorb 103. Two samples were needed for a complete analysis of an outlet sample of the reactor. Calibration factors of the GC were obtained by using gas standards.

Table 1
Total metal dispersion and mean particle size (Pt–Ru/SiO_2)

Catalyst		D^a (%)	d Chem^b (nm)	d TEM^b (nm)
Pt (at%)	Ru (at%)			
100	–	14.7	6.9	7.9
75	25	17.5	5.7	6.5
50	50	29.3	3.4	5.1
25	75	28.7	3.3	4.2
–	100	34.5	2.8	3.5

[a] D = metal dispersion (Pt + Ru).

[b] d Chem and d TEM = mean particle size by H_2 chemisorption and transmission electron microscopy respectively.

3. Results

Table 1 shows the total metal dispersion and the mean particle size determined by chemisorption and CTEM. A reasonable agreement is noted between the particle size obtained by the two methods. The results show that the particle size decreases with increasing Ru/Pt ratio, with the average particle size being the smallest in the monometallic Ru/SiO_2 catalyst. Fig. 1 shows the particle size distribution of the whole catalyst series. Fig. 2a shows a low-magnification electron micrograph of the sample $Pt_{50}Ru_{50}$ as an example of the bimetallic

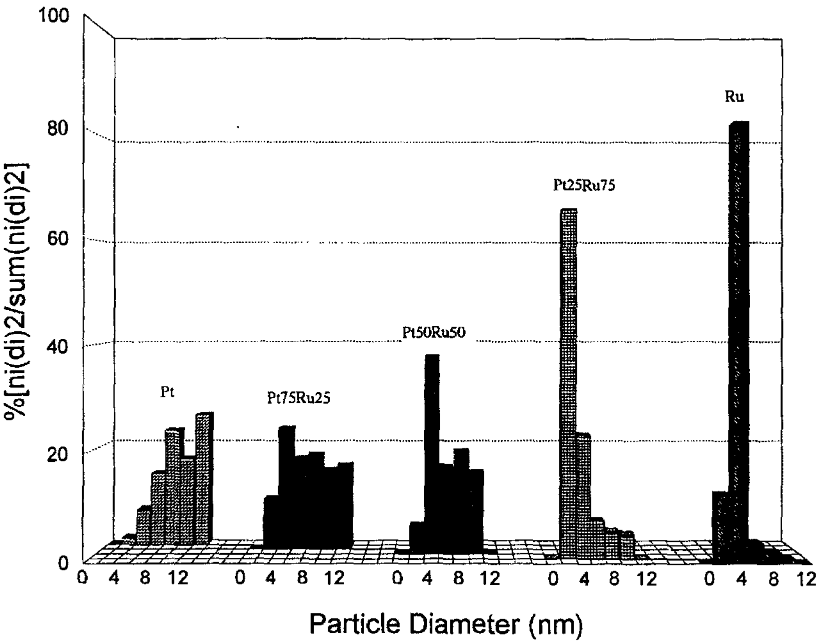

Fig. 1. Particle size distribution of Pt, Ru and Pt–Ru catalysts supported on SiO_2.

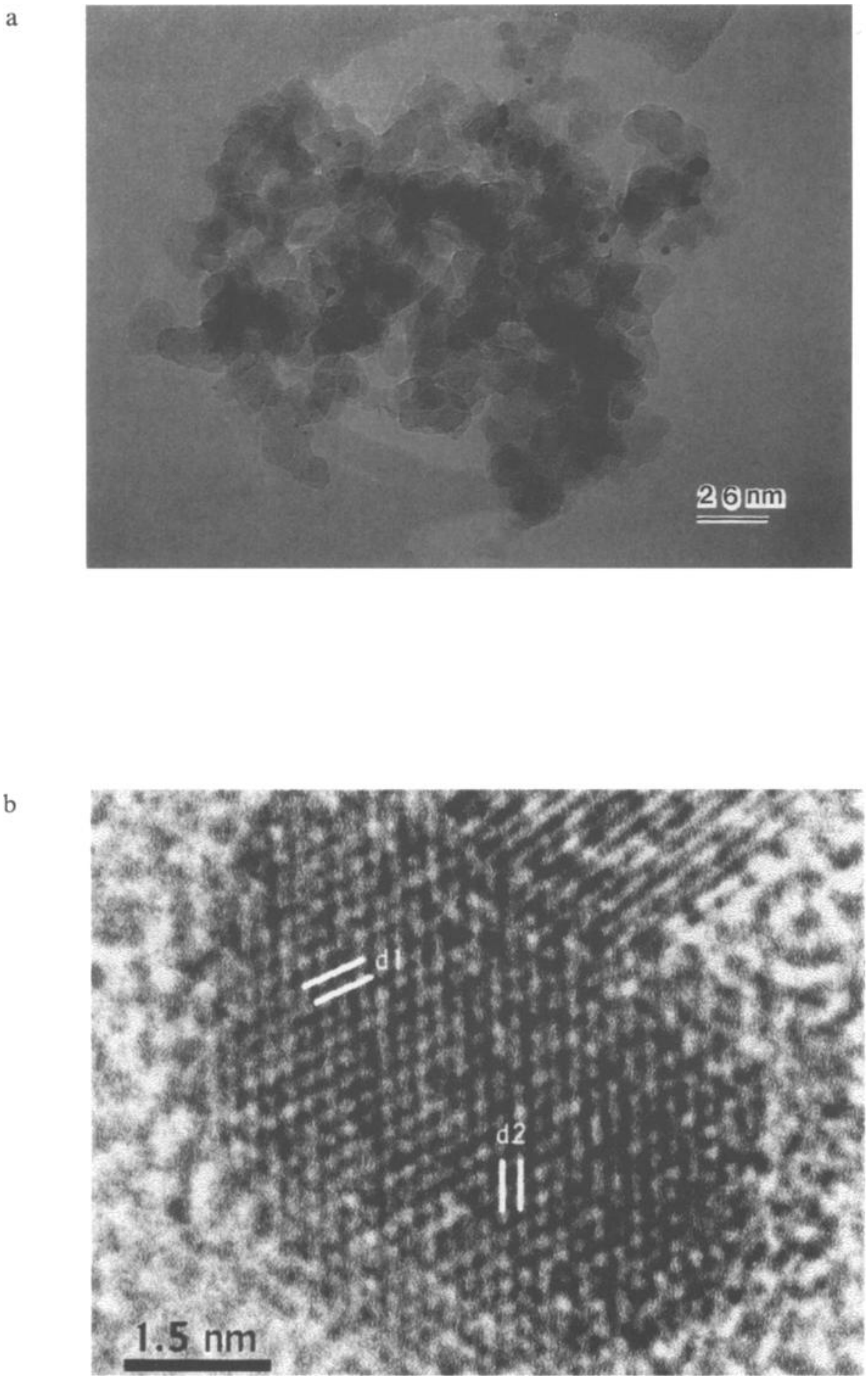

Fig. 2. (a) Low-magnification TEM micrograph showing a general view of the $Pt_{50}Ru_{50}$ bimetallic catalyst. (b) Selected particle of the same catalyst showing lattice and atomic resolution. (c) EDX microanalysis of one particle in the $Pt_{50}Ru_{50}$ catalyst. (d) HRTEM micrograph of another area of the same catalyst showing very small particles. (Continued on next page.)

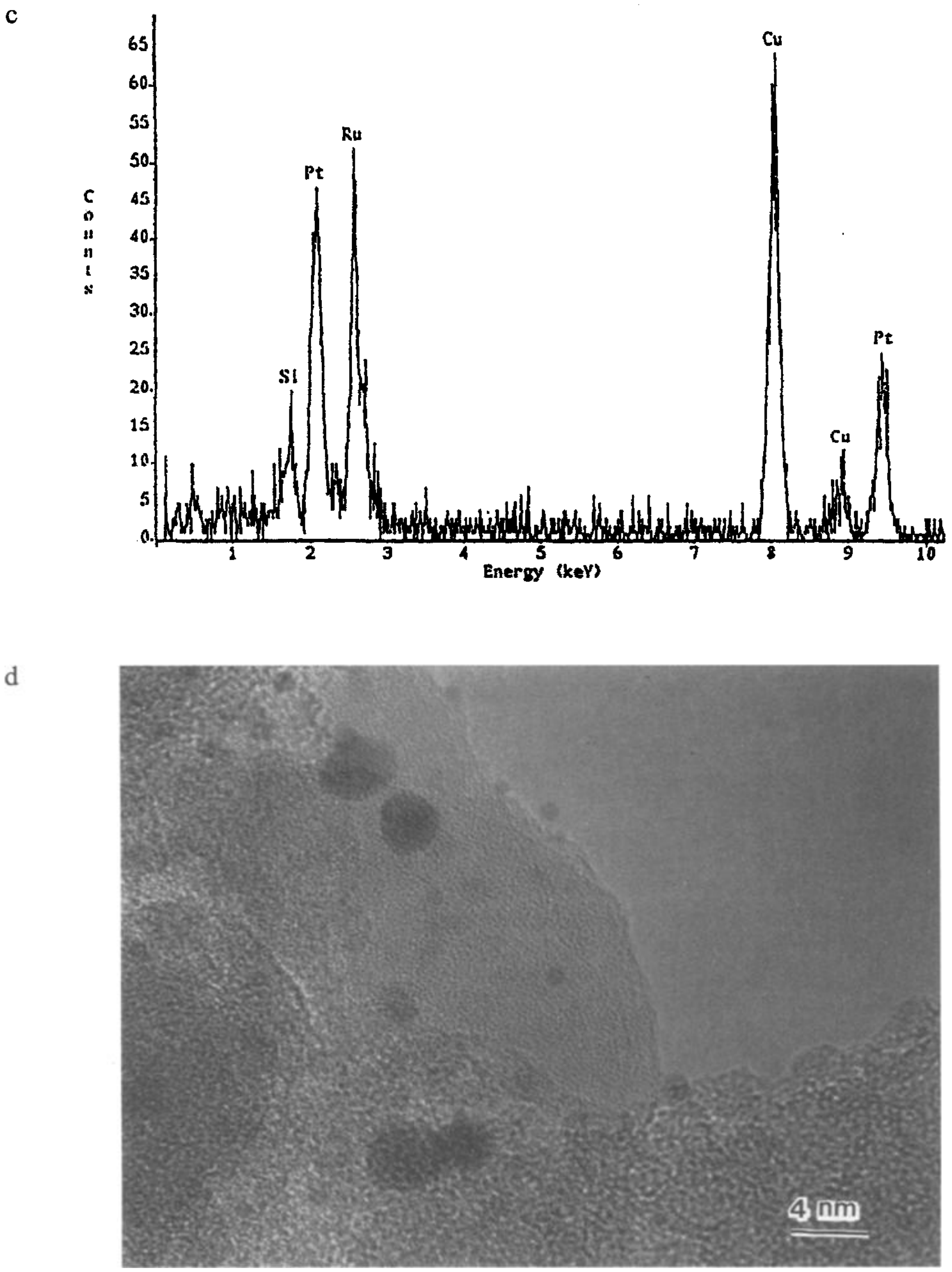

Fig. 2. (Continued.)

catalysts. Detailed examination of the image indicates the presence of several metallic particles with various shapes and sizes. Most of the particles have the shape shown in fig. 2b, with an fcc structure. Measurements of fringe spacings from the micrograph ($d_1 \approx 0.22$ nm and $d_2 \approx 0.19$ nm) indicate values close to the $d_{(111)}$ Pt and $d_{(002)}$ Pt spacings respectively. A particle by particle EDX microanalysis was performed on particles of the type seen in fig. 2b for the $Pt_{50}Ru_{50}$ catalyst. The results indicated the presence of bimetallic (Pt–Ru) particles (fig. 2c). In addition, quantitative analysis revealed that the bimetallic particles have a tendency to form Pt-rich particles. In other regions of the same sample, a second interesting type of particle was detected, having a mean size of about 0.5 nm (fig. 2d). No EDX measurements were carried out on such particles, however we suggest that this type of particle might be pure Ru clusters composed of a few metal atoms. Recently, a similar result has been reported in the study of ruthenium monometallic and bimetallic catalysts, where Ru clusters of no more than twelve atoms were evidenced using EXAFS [7].

The overall NO conversion as a function of the reaction temperature for the Pt, Ru and Pt–Ru samples is shown in fig. 3. The platinum monometallic catalyst is very active with NO conversion of 100% at temperatures as low as 398 K. The Ru catalyst is less active and complete conversion is only observed at 673 K. The plots of the bimetallic samples show generally a lower activity compared to the Pt sample, but a significantly higher

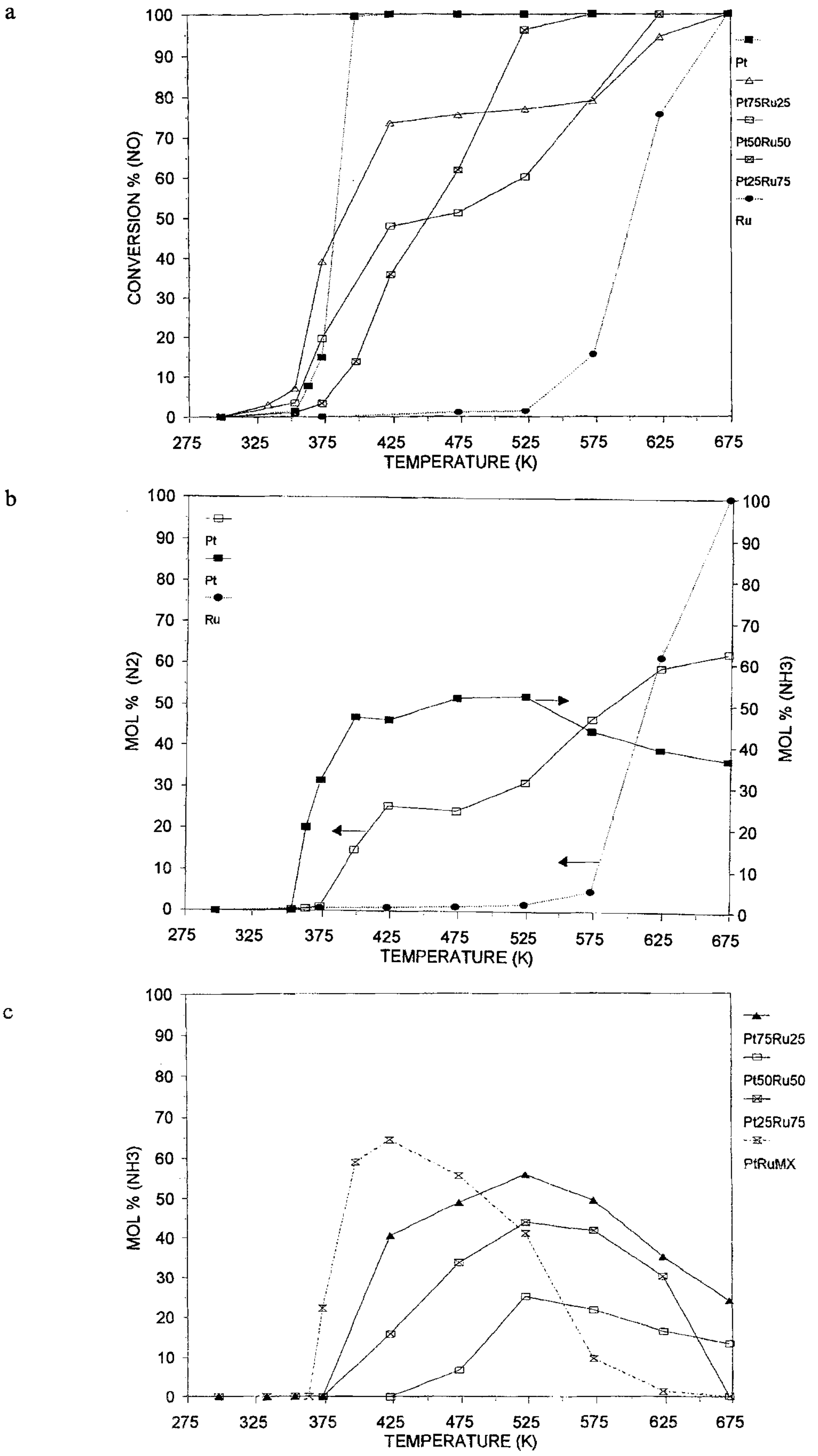

Fig. 3. (a) Overall NO conversion for the Pt, Ru and Pt–Ru catalysts. (b) Product distribution (N_2 and NH_3) as a function of the reaction temperature for Pt and Ru catalysts. (c) Ammonia distribution for the bimetallic Pt–Ru samples and a mechanical mixture of the pure phases (PtRuMX). (d) Nitrogen distribution. (e) Nitrous oxide distribution. (Continued on next page.)

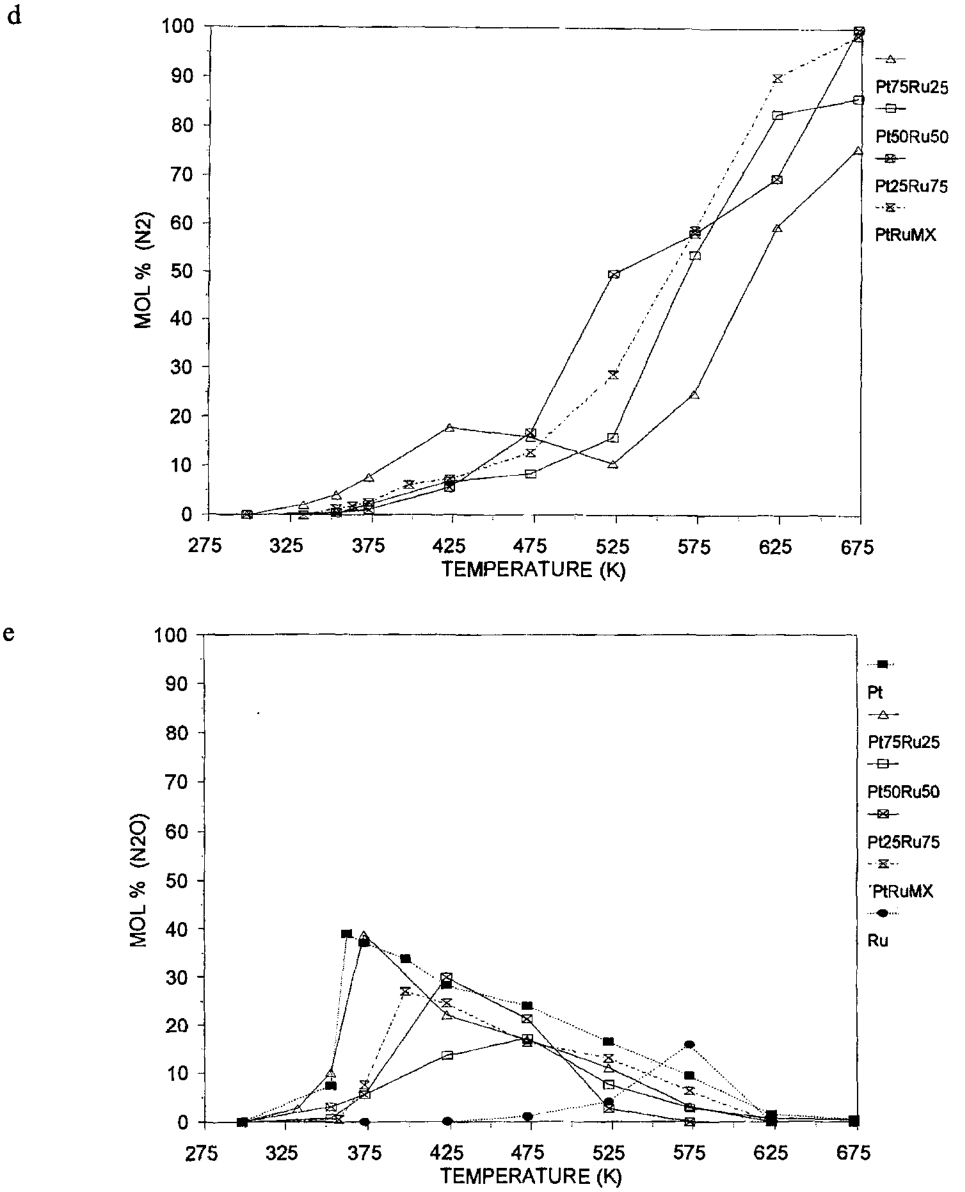

Fig. 3. (Continued.)

activity when compared to the Ru sample. It is interesting to note that the overall activity of the bimetallic samples seems to follow the nominal composition of the catalyst.

The products observed at the outlet of the reactor were: residual NO (unreacted), NH_3, N_2O, N_2 and H_2O. The selectivity for each component has been determined by $\%\mathrm{mol}C_i = C_i/\sum C_i$. The mol% of NH_3, N_2O and N_2 produced, was plotted as a function of the reaction temperature for Pt, Ru and Pt–Ru catalysts. The behaviour of the monometallic catalysts is shown in fig. 3b. These results show that the product distribution is significantly different on each sample; NH_3 production is very high on Pt and almost constant during all the run while on Ru, it is not observed. On both catalysts, Pt/SiO_2 and Ru/SiO_2, the N_2 selectivity increases with the reaction temperature but on Pt, the production of this component is only about 60% while on Ru it reaches 100% at 673 K.

Fig. 3c shows the NH_3 yield for the Pt–Ru bimetallic samples. The amount of NH_3 produced by the $Pt_{75}Ru_{25}$ is similar to that observed for the pure Pt catalyst (fig. 3b); the plot for the $Pt_{25}Ru_{75}$ sample is slightly different, showing a complete disappearance of this product at 675 K. The $Pt_{50}Ru_{50}$ catalyst behaves differently. At 523 K, the NH_3 production is the lowest (25%) of the four bimetallic catalysts and then a smooth decrease is observed up to 673 K. The mechanical mixture PtRuMX shows the highest NH_3 production at low temperatures with a sharp decrease until complete disappearance at 675 K. For the whole series of bimetallic catalysts, the N_2 production increases as a function of the Ru concentration in the catalyst, fig. 3d.

Regarding the N_2O formation (fig. 3e), the general trend in the whole series indicates that N_2O is an initial product. The maximum concentration of this product (~ 40 mol%) is observed for Pt and the $Pt_{75}Ru_{25}$ catalysts at 350 K. As the Ru concentration in the catalyst increases, the amount of N_2O produced decreases with a concomitant increase of the temperature at which the highest concentration of this product is observed. The evolution of this product on the PtRuMX catalyst is similar to that observed on the $Pt_{25}Ru_{75}$ catalyst. On the other hand, in the whole series, the N_2O concentration decreases until total disappearance as the reaction temperature increases.

4. Discussion

Ru has an exceptional selectivity for N_2 formation compared to Pd, Pt, and even Rh. Therefore, it is not surprising that studies concerning the NO interaction with Ru and Pt single crystal surfaces indicate a basic difference in the NO chemisorption on these metal surfaces. The literature regarding the NO adsorption on Ru surfaces has provided considerable data to help understand its selectivity [8–11]. On Ru(101) for example, NO is primarily adsorbed associatively at 300 K and it has been suggested that the dissociation reaction may be sensitive to the surface structure. The high selectivity for N_2 formation in the catalytic reduction of NO with H_2 and CO on supported Ru catalysts compared to Pt and Pd catalysts has been explained primarily as a result of the strong NO chemisorption over Ru which tends to increase the probability of adjacent N-species pairing and thus the formation of N_2 [12,19]. In addition, the adsorption of NO on Ru($10\bar{1}0$) followed by LEED and AES analyses has shown that the NO rapidly dissociates on the Ru surface and forms separate nitrogen and oxygen islands. At moderate temperatures, N_2 is readily desorbed leading to a buildup of oxygen and finally a cessation of NO dissociation. If, however, H_2 or CO are present, the adsorbed oxygen can be removed allowing the continuous dissociation of NO and evolution of N_2 [8]. The hydrogenation of nitric oxide on (001) and (1,1,10) surfaces of ruthenium has shown under conditions of an excess of H_2 at 450 K, that the rate of N_2 formation on the stepped Ru (1,1,10) surface is one order of magnitude faster than that on the flat (001) surface [13].

On Pt, the activity for the NO adsorption varies significantly with the topology of the exposed surface with the (410) stepped surface presenting an unusual activity for the breaking of the N–O bonds. In general the trend for the relative activity for NO dissociation on Pt surfaces varies as follows: Pt(410) > Pt > polycrystalline > Pt(100) > Pt(110) > Pt(111) [14].

The influence of the surface structure on the selectivity in the NO–H_2 reaction for Pt–Rh alloy single crystal surfaces has been stressed by Siera et al. [15] and Hirano et al. [16]. The selectivity varies drastically with the surface structure; the N_2/NH_3 ratio increases in the following order (111) < (100) < (410) which is the same finding for the N–O bond scission activity. Taking into account the elementary steps of the reaction scheme in the reduction of NO by H_2 that have been proposed, the authors conclude that the selectivity of the NO–H_2 reaction seems to be determined by the relative concentration of N, H and NO on the surface. Therefore, the structure and composition of the Pt–Rh alloy catalysts should affect the relative importance of each of the proposed reaction pathways and determine in this way the selectivity of the reaction. Platinum-rich surfaces would therefore promote the enhancement of the adsorbed species which leads to the N_2O and NH_3 products, while Rh-rich surfaces would be more selective towards N_2 formation.

Our particular interest in this study is the catalytic behavior of the bimetallic Pt–Ru catalysts. Two points will be undertaken: the understanding of the overall activity on one side, and the selectivity of the catalysts compared to that of the pure Pt and Ru catalysts on the other.

It is well established that the absolute amount of the different reaction products formed during the reduction of NO by H_2 varies according to the reaction conditions, e.g. catalyst, support, gas composition and temperature [17]. The results under our experimental conditions have shown that NH_3 is not produced (or produced in quantities that are below our detection limit) on the Ru monometallic catalyst and that only small quantities of N_2O are present. This agrees with the general characteristic behavior of Ru catalysts [17,18]. On the other hand, the selectivity of Pt to promote the reduction of NO to N_2 rather than to NH_3 is poor, especially at low temperatures [19] which is actually observed in our case.

As shown in fig. 3, all the catalysts have a rather good overall activity for the NO–H_2 reaction following the general order: Pt > Pt–Ru > Ru. It is interesting to note that the activity curve (fig. 3) for the bimetallic Pt–Ru samples mostly follows the Ru nominal composition in the catalyst; the addition of Ru, which is "non-active" at lower temperatures (< 525 K), results in a drop of the overall activity of the Pt catalyst. The bimetallic catalysts have shown a very interesting selectivity towards NH_3 formation, this being considerably lower than that observed for pure Pt. For the whole series, at the highest temperature, this selectivity varies as follows Pt > $Pt_{75}Ru_{25}$ > $Pt_{50}Ru_{50}$ > $Pt_{25}Ru_{75}$. On the other hand, the selectivity towards N_2 on the Pt–Ru bimetallic samples is higher compared to that observed on the Pt catalyst.

These results indicate that the surfaces responsible for the observed catalytic behavior have, a forciori, a different atomic arrangement from that of a pure metal, with a high probability of the occurrence of a mixture of Pt–Ru surfaces. In the following, a detailed argumentation of this latter is proposed. From a physical point of view, the substitutional solid solution of Ru atoms in the Pt lattice is possible since the atomic radii of these two atoms (0.137 nm for Pt and 0.132 nm for Ru) do not differ more than 15%, which satisfies the Hume–Rother empirical size rule for the occurrence of solid solutions [20]. However, the solid solution to be formed would not be a stable compound of definite chemical proportions because of the equivalent electronegativity of the Pt and Ru atoms. Even if we assume that all nearest-neighbor atoms of Pt should be Ru and vice versa, which is equivalent to the formation of a Pt–Ru alloy having the bcc structure, the structure is nevertheless not favored electronically because of the repulsive interaction between the two atoms. This electronic effect rather leads to the formation of a disordered Pt–Ru alloy, or the so-called *two-phase* system in which Pt-rich and Ru-rich phases are likely to crystallize in a system other than the bcc. The above physical considerations seem to agree with the fact that fcc features are observed on HRTEM images, and with the EDX microanalysis which indicates the presence of Pt-rich particles. With all these arguments in mind, we may say that we are making a clear evidence of the formation of an fcc disordered bimetallic Pt–Ru alloy, having the unit-cell parameter *a* close to that of Pt.

Theoretically, four site types; namely (0,0,0), (1/2,1/2,0), (1/2,0,1/2) and (0,1/2,1/2) determine the basic fcc system. To form a Pt–Ru alloy rich in Pt, we must at most substitute one Pt atom with a Ru one in a given unit cell. A disordered alloy can be formed therefore by inverting randomly in each neighboring unit cell the site type of the Ru atom. On this basis, the particle model presented in fig. 4 has been constructed, where white dots represent Pt atoms and dark dots the Ru ones. A rough particle has been chosen to be close to a real particle shape as it has already been evidenced by previous HRTEM studies [21]. Different types of surfaces can be recognized including those with pure Pt atoms and Pt–Ru surfaces mixture. Now, let us more closely examine how the above Pt–Ru model can help understand the activity and selectivity of the Pt–Ru catalysts.

The activity of the Pt–Ru bimetallic catalysts is shown to be lower than that of the pure Pt catalyst. As seen

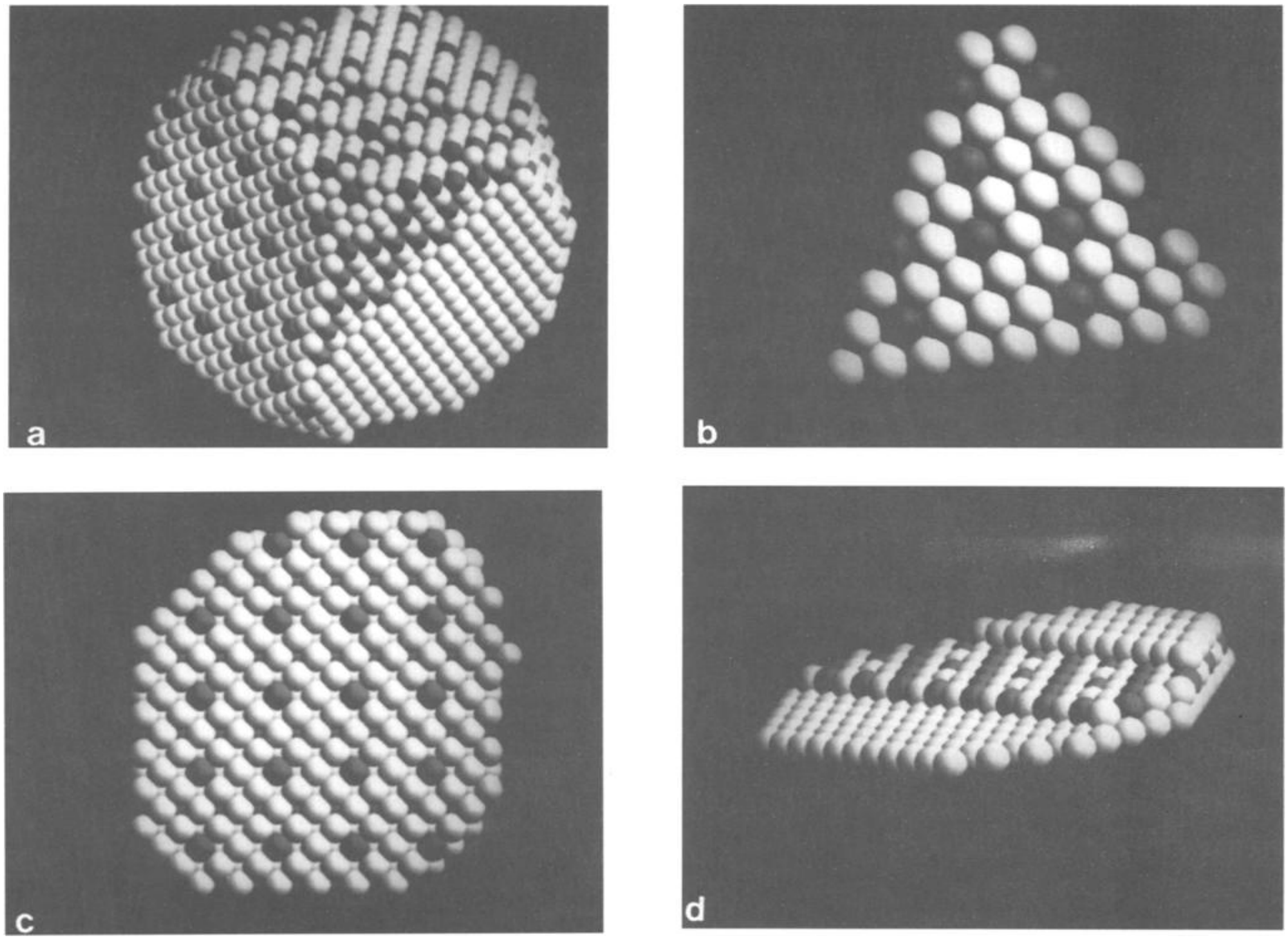

Fig. 4. (a) Model PtRu particle assuming a Pt-rich composition. White dots represent Pt atoms and gray dots represent Ru atoms; (b) (111) (c) (110) and (d) (410) type exposed surfaces.

before, the activity of Pt surfaces towards NO dissociation which is usually found to be the rate determining step in most NO reactions is structure sensitive. There is a clear evidence from experimental works [15] that the Pt activity for this reaction increases in the surface order (111) < (110) < (100) < (410). Therefore, the activity of a Pt particle during the NO reduction by H_2 must be related with the presence and accessibility to those kinds of surfaces. Figs. 4b, 4c and 4d show respectively the (111), (100) and (410) surfaces present in the model particle shown in fig. 4a. We can observe that most of the surfaces include arrangements of Ru atoms which could influence the intrinsic activity of the Pt planes and therefore be responsible for the lower activity in the Pt–Ru catalysts. The fact that the catalytic activity of the bimetallic samples at lower temperatures is closer to that of pure Pt is possibly related to the presence of a large amount of Pt-rich surfaces. This could indeed be the case in the $Pt_{75}Ru_{25}$ bimetallic catalyst. On the other hand, the catalytic behavior of the $Pt_{50}Ru_{50}$ sample suggests that the number of Pt-rich surfaces may be lower in this case. When the Ru concentration in the catalyst increases as for the $Pt_{25}Ru_{75}$ sample, the probability for the ocurrence of Pt-rich surfaces may decrease, being possible to think in the simultaneous presence of Pt particles and Ru-rich or pure Ru particles.

The same argument can be applied to understand the selectivity towards NH_3 and N_2 observed in the bimetallic catalysts. Pure Pt surfaces will promote the formation of N_2O and NH_3 while on pure Ru surfaces the selectivity towards N_2 must be very high. In the latter, the highest selectivity of the catalyst is correlated to the increase of the Ru plane atomic density which leads to a maximum amount of adsorbed nitrogen atoms. For Ru, the model shows that in general, surfaces do not expose a high density of Ru atoms, therefore, the probability of N-species pairing for the N_2 formation will decrease as compared to pure Ru surfaces and, on the other hand, the occurrence of a mixture of these Pt–Ru surfaces in the particle as shown in fig. 4 could certainly influence the relative concentrations of N, O, H and NO on the surface to determine in this way the selectivity of the reaction. On the $Pt_{75}Ru_{25}$ catalyst, the presence of Ru dense planes is not very likely to occur which would explain the product distribution; on the $Pt_{50}Ru_{50}$ sample, the exposed Pt–Ru mixed surfaces might be the highest and on the $Pt_{25}Ru_{75}$ catalyst the occurrence of Ru dense planes would certainly increase which could explain the high amount of N_2 produced and the complete disappearance of ammonia. This argument seems to explain also the singular behavior of the PtRuMX sample.

5. Conclusions

In the present work we have shown the catalytic behavior of Pt, Ru and Pt–Ru silica supported catalysts for the NO reduction by hydrogen in the temperature range 298–673 K. The physical characterization by HREM techniques has evidenced the occurrence of truly bimetallic particles with a tendency to form Pt-rich particles. The overall activity of the pure phases agreed with that reported in the literature and for the bimetallic catalyst in the temperature range of 375–525 K, the behaviour suggested a "dilution" of the active component at this temperature (Pt). The product distribution for the bimetallic catalysts indicated on the other hand a better selectivity towards N_2 formation with a significant decrease in the selectivity for the ammonia product.

A model of a bimetallic Pt–Ru particle was proposed in which some exposed surfaces allow to explain the activity and selectivity of the bimetallic catalyst. Arrangements of Ru atoms on the particle surfaces could influence the intrinsic activity of the Pt planes and therefore be responsible for the lower activity in the Pt–Ru catalysts. On the other hand, the occurrence of these Pt–Ru surfaces mixture in the particle could certainly influence the relative concentration of N, O, H and NO on the surface to determine in this way the selectivity of the reaction.

Acknowledgement

This research was supported by CONACYT. The authors wish also to thank JEOL Japan for making available to us the use of a JEM 2010F electron microscope for the analytic analysis of a sample. We are also grateful to: Professor J.L. García Fierro for stimulating discussions, Dr. Sergio Fuentes for his critical review of the manuscript, Mr. Samuel Tehuacanero for the image processing, Mr. Alfredo Sánchez and Mr. Pedro Mexia for photographic help and Mr. Luis Rendón for the HREM images.

References

[1] G.L. Bauerle and K. Nobe, Ind. Eng. Chem. Prod. Res. Dev. 13 (1974) 185;
M. Shelef and H.S. Gandhi, Ind. Chem. Prod. Res. Dev. 11 (1972) 2.

[2] W.E. Bell and M. Tagami, J. Phys. Chem. 67 (1963) 2432.

[3] R.L. Klimish and K.C. Taylor, Environ. Sci. Technol. 7 (1973) 127.

[4] S. Kim and M.J. D'Aniello Jr., Appl. Catal. 56 (1989) 23.

[5] B.R. Powell and Y. Chen, Appl. Catal. 53 (1989) 233.

[6] S. Alerasool and R.D. Gonzalez, J. Catal. 124 (1990) 204;
H. Miura, K. Tagushi, K. Sugiyama, T. Matsuda and R.D. Gonzalez, J. Catal. 124 (1990) 194;
G. Díaz, F. Garin, G. Maire, S. Alerasool and R. Gonzalez, Appl. Catal. A 124 (1995) 33.

[7] M.C. Sánchez Sierra, J. García Ruíz, M. Garzia Proietti and J. Blasco, J. Mol. Catal. A 96 (1995) 65.

[8] R. Ku, N.A. Gjostein and H.P. Bonzel, Surf. Sci. 64 (1977) 465.

[9] Thomas and W.H. Weinberg, Phys. Rev. Lett. 41 (1978) 1181.

[10] H.P. Bonzel and T.E. Fischer, Surf. Sci. 51 (1975) 213.

[11] P.D. Reed, C.M. Comrie and R.M. Lambert, Surf. Sci. 72 (1978) 423.

[12] K.C. Taylor and R.L. Klimish, J. Catal. 30 (1973) 478.

[13] T. Nishida, C. Egawa, S. Naito and K. Tamaru, J. Chem. Soc. Faraday Trans. I 80 (1984) 1567.

[14] W.F. Banholzer, Y.O. Park, K.M. Park and R.I. Masel, Surf. Sci. 128 (1983) 176.

[15] J. Siera, B.E. Nieuwenhuys, H. Hirano, T. Yamada and K.I. Tanaka, Catal. Lett. 3 (1989) 179.

[16] H. Hirano, T. Yamada, K.I. Tanaka, J. Siera, P. Cobden and B.E. Nieuwenhuys, Surf. Sci. 262 (1992) 97.

[17] T. Koylinski and B. Taylor, J. Catal. 33 (1974) 376;
W.C. Hecker and A.T. Bell, J. Catal. 92 (1985) 247.

[18] H. Muraki and Y. Fujitani, Ind. Eng. Chem. Prod. Res. Dev. 25 (1986) 414.

[19] M. Shelef and H.S. Gandhi, Ind. Eng. Chem. Prod. Res. Develop. 8 (1972) 393.

[20] W. Hume-Rothery, *Electrons, Atoms, Metals, and Alloys*, 3rd Ed. (Dover, 1963).

[21] M. José-Yacamán, S. Tehuacanero, C. Zorrilla and G. Díaz, Mater. Res. Soc. Symp. Proc. 398 (1995) 133.